A Theoretical-Empirical Approach to the Mechanism of Particle Entrainment from Fluidized Beds

F. A. ZENZ and N. A. WEIL

The M. W. Kellogg Company, New York, New York

A means of calculating the rate of entrainment of solids from commercial-size continuously operating fluidized beds was developed from the combined results of a theoretical and an empirical approach which through different channels arrived at the same fundamental mechanism. The calculation method shows agreement with data obtained from an apparatus simulating flow characteristics in large-scale equipment and compares favorably with smaller scale tests reported in the literature at pressures up to 200 lb./sq. in. gauge.

In vessels containing a fluidized-catalyst bed through which gas is forced upward, the gas leaving the top of the bed will carry with it entrained solid particles. This entrainment varies with a number of factors such as gas velocity, particle-size distribution, height above the bed, specific gravity of the catalyst, and viscosity and density of the gas. The problem is similar to that of entrainment of liquid from distillation trays wherein an optimum relation between tray diameter, number of trays, and tray spacing is used to determine the minimum-cost installation. In the case of particle entrainment in catalytic reactors, a quantitative entrainment correlation would define the relation between disengaging height, number of cyclone stages, and carryover loss, leading again to the over-all minimum-cost arrangement.

Numerous experimental investigations of entrainment in small laboratory-scale equipment have been reported, but no generally applicable empirical relationship has yet been found or proposed. Even within the work of a single investigator apparently inexplicable inconsistencies appear in the data, and some of the most ambitious studies have been able to relate results only qualitatively to the observed nature of the bubbling action in the bed. Entrainment from small-diameter, high L/D, experimental units, in which the gas bubbles within the fluidized mass may reach tube-diameter proportions, giving rise to slugging, can be expected to correlate only by coincidence with the entrainment from large-diameter commercial units, where the emerging bubbles may reach several feet in diameter but never the diameter of the entire vessel. The generalized approach developed in the present study is intended to apply only to such larger diameter nonslugging beds.

F. A. Zenz is with Associated Nucleonics, Inc., Garden City, New York.

THE MECHANISM OF CATALYST ENTRAINMENT

Two approaches to the calculation of entrainment, which upon later comparison were found to converge to a common physical mechanism, are illustrated in Figure 1.

The theoretical approach in Figure 1(a) envisioned particles ejected from the bed surface (at a velocity of the magnitude of the bubble velocity as it bursts through the bed surface) into a concurrent stream of gas rising uniformly at a rate equal to its superficial velocity through the bed. Each particle thus thrust into the gas is then acted upon by inertia and gravitational and drag forces. Some sizes will be carried up continually and some only to certain heights, from which they will fall back onto the bed. Thus a theoretical analysis of this picture results in a curve of concentration versus height above the bed surface for any particular catalyst gas system and operating gas rate.

The empirical approach pictured in Figure 1(b) envisioned the bed as a saturation feed device such that at a sufficient distance above the bed surface (where gas-velocity profiles have stabilized) the containing vessel can be considered as a pneumatic conveying tube and entrainment as a transport phenomenon. It was hypothesized that gas bubbles bursting at the surface of a fluidized bed are analogous to intermittent jets imposing a highly irregular velocity profile across the containing vessel. The jet velocities eventually are dissipated to the superficial gas velocity at some equilibrium height above the bed surface referred to as the *transport Disengaging height, T.D.H.* The entrainment above this height is then relatively constant and presumably equal to the maximum or saturation dilute-phase particle-carrying capacity of the gas stream at its superficial velocity as obtained from empirical correlation of pneumatic and hydraulic transport data.

THE THEORETICAL APPROACH THROUGH FORCES ACTING ON THE PARTICLES

In order to approach the conditions acting on catalyst particles entrained above the bed in process vessels, the behavior of the particles in a moving gas stream must be considered. The motion of any one such particle, with any inter-particle forces neglected, is completely described by the equation

$$\text{inertia force} + \text{gravitation force} + \text{drag force} = 0$$

or, in mathematical terms, upward vectors being considered as positive,

$$m\frac{dv}{dt} + F = -mg\frac{\rho - \rho_0}{\rho} \qquad (1)$$

where the right-hand side represents the effective particle weight.

The initial particle velocity as it is thrown upward from the bed surface by the violent action of bursting bubbles is represented as v_0. However, as soon as it leaves the bed it immediately enters a gas mass flowing at a uniform velocity v_g representing the superficial velocity of the rising process gas above the bed surface. The drag force in Equation (1) can be expressed as $F = C_R R$, where for streamline or laminar motion

$$C_R = k\mu/D\rho_0(v - v_g)$$

and

$$R = \rho_0(v - v_g)^2 A/2$$

so that by substitution

$$F = k\mu A(v - v_g)/2D$$

Equation (1) may now be rewritten as

$$\frac{dv}{dt} + \frac{k\mu A}{2mD}(v - v_g) = -g\frac{\rho - \rho_0}{\rho} \qquad (2)$$

If the particles are assumed to be spherical, then

$$A = \pi D^2/4$$

and

$$m = \rho\pi D^3/6$$

so that

$$\frac{2mD}{k\mu A} = \frac{4\rho D^2}{3k\mu} = C \qquad (3)$$

Substituting Equation (3) in Equation (2) and applying the boundary conditions that $v = v_0$ at $t = 0$ yields the solution of

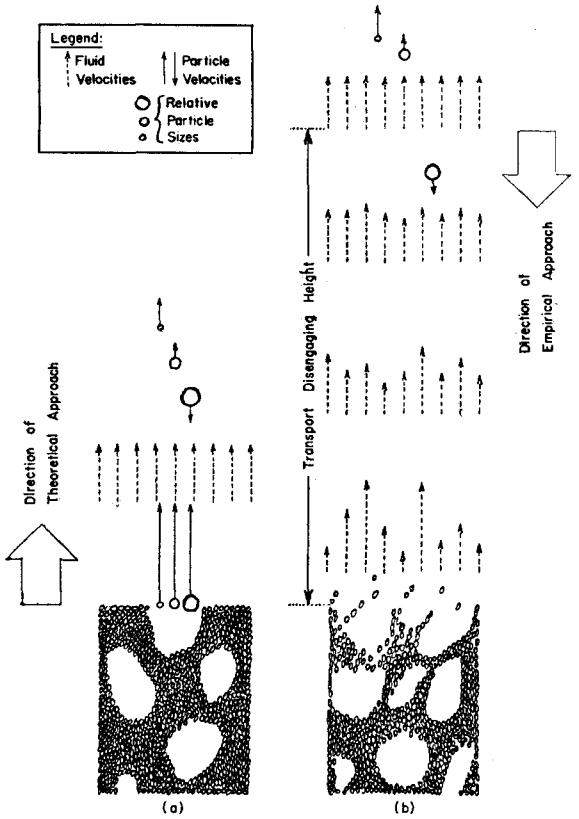

Fig. 1. Illustrations of assumed flow models.

Equation (2) (ρ_0 being assumed negligible with respect to ρ) as

$$v = (C_g - v_g)(e^{-t/C} - 1) + v_0 e^{-t/C} \quad (4)$$

The balancing velocity (v at $t = \infty$) is then

$$v_m = -C_g + v_g \quad (5)$$

which substituted into Equation (4) gives

$$v = v_m(1 - e^{-t/C}) + v_0 e^{-t/C} \quad (6)$$

At the point of maximum vertical rise $v = 0$, and so from Equation (6) the time for reaching the top elevation is

$$t^* = C \ln\left(1 - \frac{v_0}{v_m}\right) \quad (7)$$

The height of rise can be calculated from the expression

$$h = \int_0^t v\, dt = \int_0^t [v_m t + (v_0 - v_m)e^{-t/C}]\, dt$$

which upon integration with the boundary condition that $h = 0$ when $t = 0$ yields

$$h = v_m t - C(v_0 - v_m)(e^{-t/C} - 1) \quad (8)$$

Substituting Equation (7) into (8) for the elapsed time gives the maximum height of rise for the particle:

$$h_{max} = C\left[v_0 + v_m \ln\left(1 - \frac{v_0}{v_m}\right)\right] \quad (9)$$

For irregular particles, k in Equation (3) has a value of approximately 37.5, which upon substitution in Equations (5), (6), and (9) gives

$$v_m = v_g - 1.15\rho D^2/\mu \quad (10)$$

$$v = (v_0 - v_m)\exp\left(\frac{-28.1\mu t}{\rho D^2}\right) + v_m \quad (11)$$

$$h_{max} = \frac{\rho D^2}{28.1\mu}\left[v_0 + v_m \ln\left(1 - \frac{v_0}{v_m}\right)\right] \quad (12)$$

If n represents the number of particles of a given grain size D thrown up by the bubble action over an area of 1 sq. ft. of the bed/sec., then $N = \sum n$ represents the average of the total number of all particles emerging from the bed per square foot per second. If the particle velocity is v at an arbitrary height, a particle having crossed a section will have traveled a distance of v feet upward in 1 sec. Since no particles are destroyed, during this 1 sec. n additional particles will have entered the 1 sq. ft. area. Hence, in a space of 1 cu. ft. there will be

$$E = n/v \quad (13)$$

particles of size D, where E denotes the entrainment of particles continuously carried up by the gas stream. However, those particles thrust upward from the bed surface and falling back thereon must also be considered. Therefore,. n may again represent the number of rising particles of a given grain size passing a 1 sq. ft. section/sec. at any arbitrary elevation h. If at this elevation their velocity is v, and it takes $\bar{t}$ sec. for the particles to complete their rise to the maximum height and to fall back to the same elevation, then the number of particles above this elevation will be

$$m = n\bar{t} \quad (14)$$

However, the difference between the total number of particles existing above two successive elevations separated by a vertical distance dh will express the entrainment volumetrically in a cube of 1 sq. ft. base and a height of dh:

$$E = \frac{m(h) - m(h + dh)}{dh} = -\frac{dm}{dh} \quad (15)$$

From Equation (14)

$$\frac{dm}{dh} = n\frac{d\bar{t}}{dh}$$

which substituted in Equation (15) gives

$$E = -n\frac{d\bar{t}}{dh} \quad (16)$$

While Equations (14) and (16) appear relatively simple, the real problem is to express E as a function of height above the bed or, in other words, v and dt/dh as functions of h. Equations (6) and (8) give v and h as functions of t; it is also possible to express h solely in terms of v according to the relation

$$h = C\left[v_0 - v + v_m \ln\frac{v_0 - v_m}{v - v_m}\right] \quad (17)$$

To obtain the $v = v(h)$ function would require inverting Equation (17). This cannot be done in closed form since this equation is of a general transcendental form. Hence, corresponding values of the $v = v(h)$ function must either be obtained by iteration from Equation (17) or by a cross plotting of Equations (6) and (8). A similar situation exists with regard to the quantity dt/dh, which must also be solved by numerical analysis.

In Equations (14) and (16) n designates the number of particles of a given grain size thrust from the bed surface by bursting bubbles, as averaged out over 1 sq. ft. of the bed/sec. In this sense $N = \sum n$ represents the entrainment value immediately at the bed surface. This is arbitrarily taken as 100 times a constant, and so

$$N = 100K = K\sum \bar{n}$$

where it is understood that

$$\sum \bar{n} = 100; \quad \bar{n} = n/K$$

with $\bar{n}$ representing the number (or weight) percentage of a given particle size in the total bed spectrum. These considerations are sufficient to establish an entrainment curve over the height of a vessel on the basis of 100 grains liberated on the average/(sq. ft. of bed surface)(sec.). This entrainment curve can be converted into the actual curve through multiplication by a factor of K. K must be obtained from one or the other of two boundary conditions: the actual entrainment at the bed surface or at a sufficient height above the bed

(> T.D.H.), where entrainment has become relatively constant.

The numerical calculation procedure is carried out as follows:

1. Subdivide the bed-catalyst size distribution into a number of representative grain sizes as illustrated in Figure 2(*a*).
2. Fix the values of μ, ρ, and ρ_0 and of the v_0 parameter for the initial velocity leaving the bed.
3. Calculate the balancing velocity of each of the representative grain sizes by Equation (10) and separate those particles carried by the gas stream ($v_m < 0$) and those returning to the bed ($v_m > 0$).
4. Calculate particle velocities as a function of time from Equation (6) and plot them as shown in Figure 2(*b*).
5. Calculate height of rise in terms of time from Equation (8) and plot as shown in Figure 2(*c*).
6. For particles carried by the gas stream ($v_m < 0$) a cross plot of v vs. h as shown in Figure 2(*d*) permits calculating the relative entrainments from $\bar{n}/v$ at various heights above the bed.
7. For particles returning to the bed, the residence times, or chord lengths $\bar{l}$ pertaining to given h values, permit drawing a plot of $\bar{l}$ vs. h as shown schematically in Figure 2(*e*).
8. The tangents drawn at various height to the curves of Figure 2(*e*) give values of $-d\bar{l}/dh$ as a function of h as shown schematically in Figure 2(*f*). Calculate relative entrainment through multiplication by a factor of $\bar{n}$ corresponding to the various grain sizes.
9. The entrainment curves corresponding to each of the various size fractions and to the over-all summation are illustrated schematically in Figure 2(*g*).

This theoretical approach to entrainment through particle dynamics describes the shape of the entrainment curve with height above the bed, as a function of the initial velocity parameter v_0 as well as the physical properties of the operating system. In the absolute sense it cannot predict entrainment without prior knowledge of n or v_0. If sufficient data were available for independent prediction of n, this method would serve as a powerful tool for correlating the entire entrainment gradient picture. (The particle Reynolds Numbers encountered in computing the balancing velocities in this study ranged from 0.0053 to 9.7.) The empirical approach to entrainment appears to permit such prediction of n so that the significance of the theoretical analysis becomes clearer by comparison with the empirical study.

THE EMPIRICAL APPROACH THROUGH SATURATION TRANSPORT

It is proposed that at some height above the surface of a fluidized bed, where the velocity profile of the rising fluid stream has become essentially constant, the condition of disperse-phase

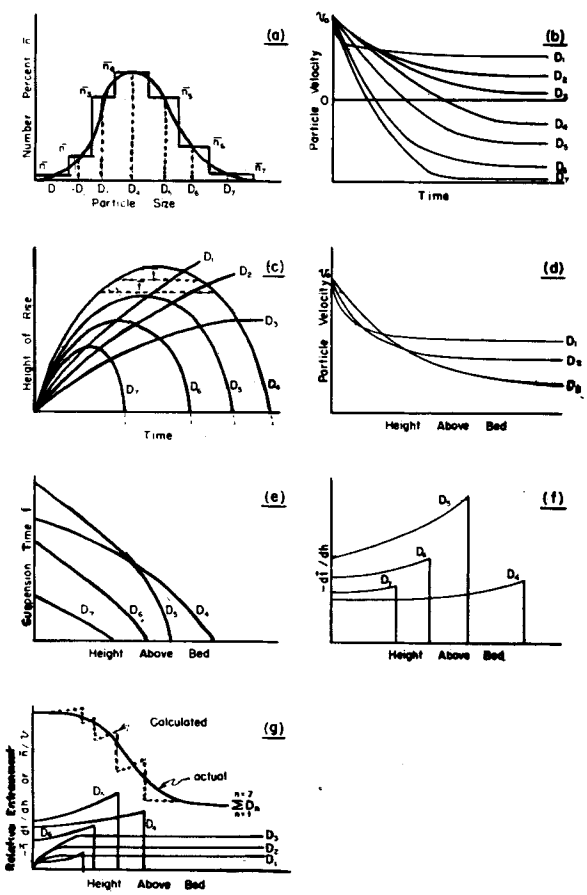

Fig. 2. Outline of stepwise procedure for calculating entrainment by a theoretical approach based on particle dynamics.

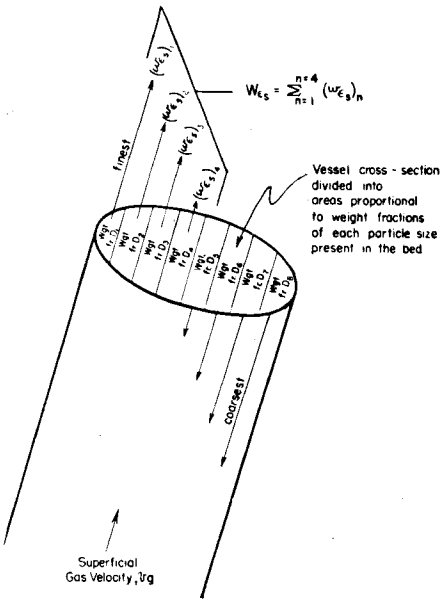

Fig. 3. Illustration of transport entrainment concept at T.D.H.

flow of entrained particles and fluid may be considered as in a carrier line or pneumatic transport line. In the experimental study of such simple vertical transfer lines, in which solids were introduced to the gas stream directly from a hopper, it was found that for a given fluid-solid system there was a maximum particle concentration that could be held in dilute static or flowing suspension. At greater densities, associations between particles caused an increase in effective particle diameter and the suspensions collapsed into slugging beds. These maximum dilute-phase concentrations defined relationships between superficial gas velocity and maximum attainable solids mass flow rate, at that gas velocity, which could be approximated by solids mass flow rate

= solids flowing density × solids velocity:

$$w_{\epsilon_s} = \rho(1 - \epsilon_s)(V_{ch} - V_{\epsilon_s}) \qquad (18)$$

Several sizes in a mixture could then be considered acting in parallel, so that

$$W_{\epsilon_s} = (f \times w_{\epsilon_s}) \qquad (19)$$

Since the saturation solids concentration coincides with the condition of incipient bed formation, it is plausible to conceive of a bed replacing the hopper as a solids feed device of relatively infinite capacity and, therefore, of saturation capacity, and so $v_g = V_{ch}$. The model then proposed for the entrainment mechanism would be envisioned as follows:

1. Large bubbles of gas pass up through the bed at velocities of a magnitude several times the balancing velocity of even the largest particle in the mixture. The bubbles erupt at the bed surface and thrust masses of solids into the space above the bed.
2. These masses of solids ejected from the

bed are comprised of the entire spectrum of particle sizes constituting the bed catalyst and contain each component size in the same quantitative distribution as in the bed proper.

3. The intermittent high-velocity bursts of gas impose a fluctuating and highly irregular time-dependent velocity profile over the cross section of the vessel. At successively higher levels above the bed surface, the velocity profile becomes more and more stable, until at and above some finite height the profile remains essentially constant, for example, the rate of change of velocity of all streamlines intersecting any cross-sectional horizontal plane approaches zero. This height has been variously referred to as the transport disengaging height, T.D.H., or equilibrium disengaging height.

4. For any given system the average velocity at T.D.H. may be considered the operating superficial velocity through the vessel. Also at T.D.H. all particles having a balancing velocity greater than the superficial velocity will already have dropped back into the bed. The remaining particles will constitute the entrained material, W_{ϵ_s}.

5. At T.D.H. the vessel cross section may be considered as divided into sections, each of which has an area proportional to the weight fraction of one component particle size of bed catalyst, in other words, a bundle of transport tubes operating in parallel each at the bed superficial velocity, v_g, as pictured in Figure 3. The bed, acting as a saturation feeder, can supply the component particle sizes to each of these channels at the maximum rate w_{ϵ_s} that the gas can transport.

6. At and above T.D.H. the total entrainment, W_{ϵ_s}, is the summation of the component saturation rates w_{ϵ_s}.

7. From the bed surface up to the value of T.D.H. the effective velocity dissipates from the surface value of the bubble velocity to the superficial velocity.

The quantitative application of this suggested entrainment mechanism requires means of computing (1) the dilute-phase saturation carrying capacity of a gas stream; (2) the transport or equilibrium disengaging height, T.D.H.; and (3) the rate of effective velocity dissipation.

Equations (18) and (19) give the relation between W_{ϵ_s} and V_{ch} at saturation; however, it is not possible to solve for W_{ϵ_s} without also knowing ϵ_s and V_{ϵ_s} for each component particle size or for the effective mixture as a whole. A fairly good estimate can usually be made of V_{ϵ_s} by assuming it equal to the terminal or balancing velocity, but only meager scraps of data are available for estimating ϵ_s. The ranges of the experimental data and the corresponding voidages at saturation density calculated from Equation (18) are given in the literature (*16*). Since ϵ_s is generally in the range of 0.94 to 1.0, a slight error in this value can make a considerable difference in the value of W_{ϵ_s}. In addition, the few available data hardly provide enough basis for developing a correlation to predict ϵ_s values for various materials. An alternate empirical correlation for V_{ch} was therefore sought. Experiments had shown that the saturation carrying capacity was identical for horizontal and vertical lines if the particles conveyed were uniform in size. It was, therefore, relevant to include data for liquid-solid systems in this search, though reported investigations with such systems all were conducted in horizontal flow and never specifically performed to measure V_s; the accuracy of the data is therefore questionable in nearly all instances. Nevertheless, such data, shown in Figure 4, served as a guide in establishing the final relationship. It will be noted in Figure 4 that the slope of the curves for mixed-size materials differs quite markedly from that for uniform-size particles. Not only is this difference noted with either gas or liquid as the carrying medium, but also the slopes for either medium are almost identical. In marked contrast to the air-transport data the water experiments show little, if any, effect of particle diameter. However, the range of diameters investigated is rather limited. It hardly appears rational to suppose that no particle-diameter effect exists, since in the extreme it is obvious that a higher water velocity would be required to convey 2- to 3-in.-diameter stones than ordinary beach sand. Figure 5 presents the best empirical correlation finally accepted for the data on uniform-size particles. Since Figure 4 showed no diameter effect among the hydraulic experiments, better agreement with the correlants of Figure 5 cannot be expected. Before testing the applicability of Figure 5 in calculating entrainment from fluidized beds, the authors reevaluated a review of the entrainment data from a number of units to determine whether the transport disengaging height could be approximated quantitatively.

The transport disengaging height, T.D.H., above which the rate of decrease in entrainment approaches zero, probably represents in most instances the design optimum for location of cyclones. It appears at the present state of knowledge that this height is some function of the bed diameter and the superficial gas velocity, approximately as shown in Figure 6. The dependence on superficial gas velocity is reasonable since increase

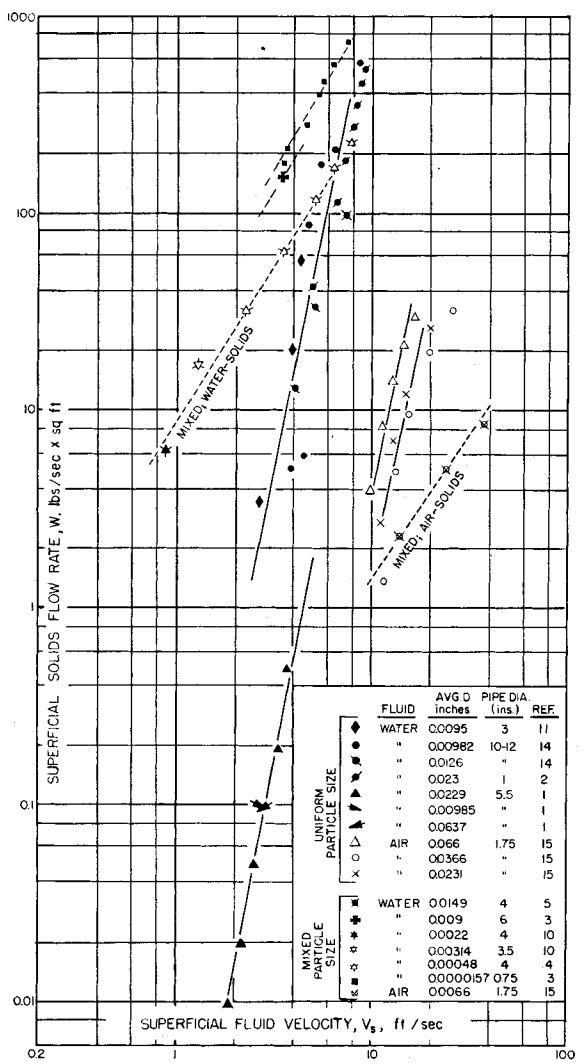

Fig. 4. Experimental saltation data in horizontal flow.

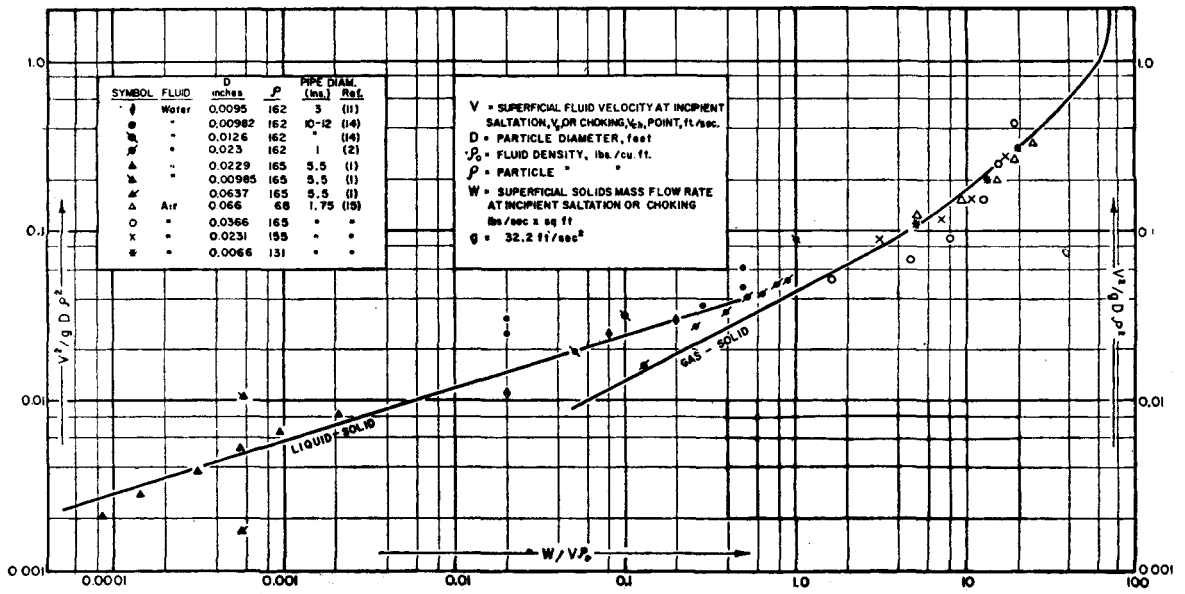

Fig. 5. Empirical correlation of saturation carrying capacity for uniform size particles in horizontal or vertical cocurrent disperse phase flow.

in velocity would increase the rate of rise, and the frequency of eruption, of bubbles at the bed surface, which would in turn require greater distance for dissipation of the fluctuating velocity profiles. The effect of bed diameter may be a result of wall effects at the low diameters and possibly poorer gas distribution at the larger diameter. Figure 6 is based on data from 2-, 3-, 8-, 12-, 24-in. and 16-ft.-diameter vessels. As these data were not obtained solely to establish a relationship for predicting T.D.H., the correlation of Figure 6 must not be considered very accurate; the data were obtained from units operating under a variety of process conditions with different inlet gas distributors and variations in particle-size analyses. The data obtained from small-diameter units may also be suspect because of slugging conditions, which impart distinctly different characteristics to the velocity profiles as well as alternate the bed level, and the effect of size segregation within the bed, which would have less import within large-diameter units, where the solids inventories are greater. Extensive laboratory entrainment experiments carried out at the M. W. Kellogg Company have shown that T.D.H. is not related to the size of the bubbles bursting at the bed surface, as might be suspected. It may, therefore, be supposed that the unstable velocity distribution resulting from small bubbles is augmented by the greater frequency of bubbles to the extent that the disengaging height required to reach a stable profile is equal to that required for large bubbles bursting more violently but less frequently.

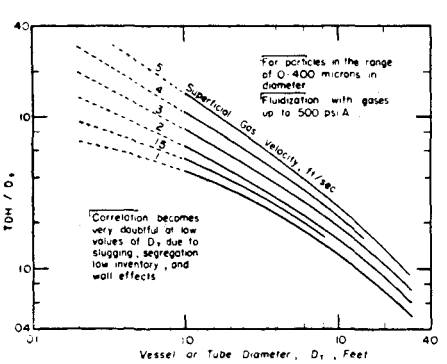

Fig. 6. Empirical correlation for estimating transport disengaging height.

To permit calculation of an entire entrainment curve the rate of effective velocity dissipation between the bed surface and the transport disengaging height must be established. In effect, the theoretical treatment of entrainment has partially bridged this gap and so it is appropriate to compare the theoretical and empirical approaches qualitatively before discussing any approximate quantitative correlations.

THE TYPICAL ENTRAINMENT CURVE

Figure 7 illustrates schematically the shape of typical experimentally determined entrainment curves and, in comparison, the extent to which the theoretical and empirical calculation methods generally approach reality. Theory predicts the relative shape of the entrainment curves but requires a quantitative boundary condition, such as, for example, the value of E at T.D.H., in order to translate the entire curve onto an absolute basis. The empirical correlation of Figure 5 could be accepted for this purpose, but theory would still fall short of observed data by too low a prediction of apparent T.D.H. This was to be expected since the maximum height of rise of particles not carried by the gas stream, with the retarding drag forces neglected, would be given by

$$\frac{(v_0 + v_g)^2}{2g}$$

For a 7 ft./sec. bubble velocity and 1 ft./sec. superficial velocity this amounts to only 1.0 ft., compared with observed values of 5 to 15 ft., depending on the vessel size. Point A can be made to coincide with point B in Figure 7 by substituting a bubble-velocity dissipation function in place of the constant superficial velocity assumed as the flow field in the original model illustrated in Figure 1(a). Such an effective velocity dissipation function would also permit carrying on entrainment calculations below T.D.H. by the empirical correlation of Figure 5.

The development of the velocity-dissipation relationship can be carried out directly by measuring velocity profiles downstream of a series of pulsating orifice jets or obtained indirectly by trial and error matching of the theory to experimental entrainment curves and calculating therefrom the required dissipation function. The former method is questionable without the presence of a bed of particles, and exceedingly difficult if not impossible with the presence of a

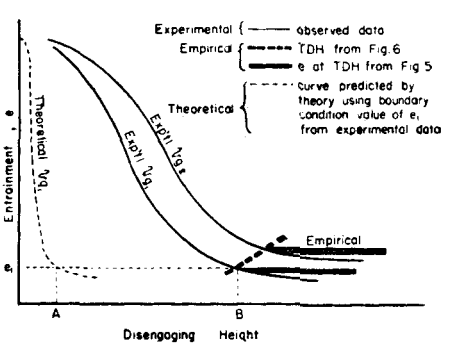

Fig. 7. Schematic comparison of theoretical and empirical entrainment calculations with experimental curve.

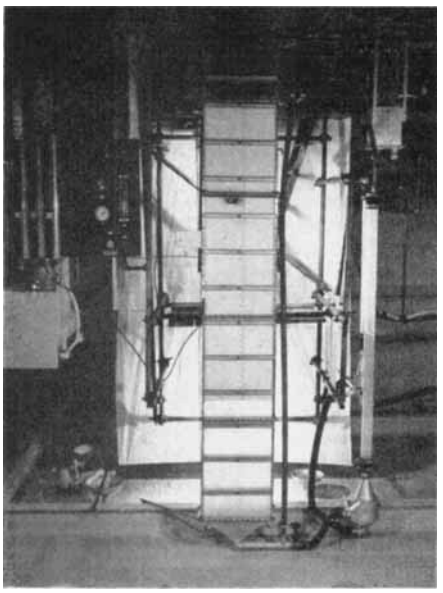

Fig. 8. Over-all view of test apparatus.

bed. The latter method is probably the most readily adapted approach; however, it requires data obtained with a system of fully defined particle-size distribution, constant bed composition (without elutriation or segregation effects), sufficient bed diameter to assure normal bubbling action without slugging tendencies, and fully determined entrainment curves extending above as well as below the transport disengaging height, in order to define exactly this reference point. Neither available commercial operating data nor small-scale experimental results were felt to be sufficiently complete in all these requirements. Attention was, therefore, focused on results obtained in an experimental apparatus particularly designed to give flow characteristics representative of commercial units, with a minimum of bulk and a maximum in bed visibility.

THE TWO-DIMENSIONAL TEST STAND

In the design of any test apparatus it is desirable wherever possible to permit observation of the physical phenomena occurring within the equipment. This is particularly true in a study of fluidization, where bed height and uniformity of flow are otherwise difficult to establish. This is also particularly difficult in fluidization studies since a single layer of particles on the surface of a transparent apparatus already renders it essentially opaque. It was, therefore, proposed to build a so-called "two-dimensional," or rectangular, apparatus simulating a differential vertical section or to slice through a 2-ft.-diameter vessel. The apparatus was made 2 by 24 in. in cross section and built of 11/16-in. thick clear Lucite. Figure 8 shows an over-all view of the test stand. The horizontal reinforcing bars were spaced approximately 1 ft. apart. With strong floodlights behind the apparatus, it was possible to observe bed levels and bed bubbling characteristics very clearly. For flexibility, especially in studying bed-depth effects, and for ease of construction, the unit was composed of five sections, namely, a bottom grid support and air distribution chamber 18 in. high, one 6-ft. and two 3-ft.-high intermediate sections, and an 8-in. triangular sheet metal cone at the top. Shop air at 60°F. and an average 100 lb./sq. in. gauge was used as the fluidizing medium, admitted through a silica gel and charcoal dryer. A two-stage external cyclone separating unit was used to separate entrained solids from the air stream. The tests were carried out in batches, the bed charge being thoroughly blended with the entrained material following each test in order to minimize bed segregation and to maintain the same composition in each run. Size analyses of the bed at the start of the tests checked with analyses made during and at the end of the program, indicating no net loss of material and a constancy of bed composition.

The size analysis of the cracking catalyst used in the tests is shown in Figure 9. The entrainment data obtained with this material are given in Table 1. Each of the recorded points represents an extrapolation to time zero for a series of measurements of entrainment rate as a function of time during a given run. These data should, therefore, not be subject to either changing particle distribution in the bed, particle-size segregation in the bed, or changing disengaging height due to loss of inventory.

COMPARISON BETWEEN CALCULATED AND EXPERIMENTAL RESULTS

It is proposed to calculate the anticipated entrainment at T.D.H. for the apparatus and solids described in Figures 8 and 9, and to compare the results with the data of Table 1. The procedure is outlined as follows:

1. At a given superficial velocity estimate T.D.H. from Figure 6 for D_T of 2 ft.
2. From the bed particle size analysis (Figure 9) make a component breakdown and tabulate the balancing velocities corresponding to each component.
3. At the superficial velocity of step 1 calculate either
   - *a.* the saturation mass flow rates w_{ϵ_s} for each component having a balancing velocity less than the superficial or
   - *b.* the saturation rate for a particle diameter equal to the geometric mean (50% point) of all particles with balancing rates less than the superficial.
4. If procedure 3*a* is followed, multiply each of the component transport rates w_{ϵ_s} by the weight fraction of the component size in the bed catalyst and summate. If procedure 3*b* is followed, multiply the calculated saturation rate by the total weight fraction of all the component sizes in the bed catalyst making up the mean D used in step 3*b*. If the catalyst analysis is

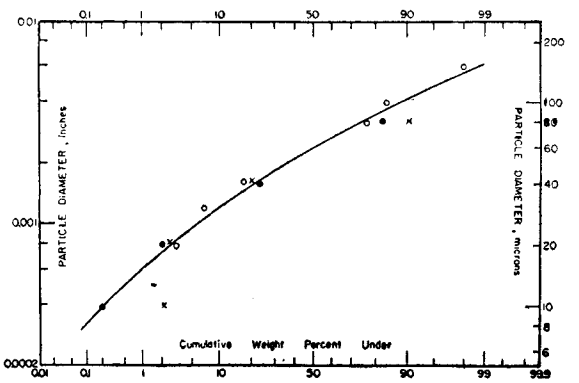

Fig. 9. Size analysis of cracking catalyst.

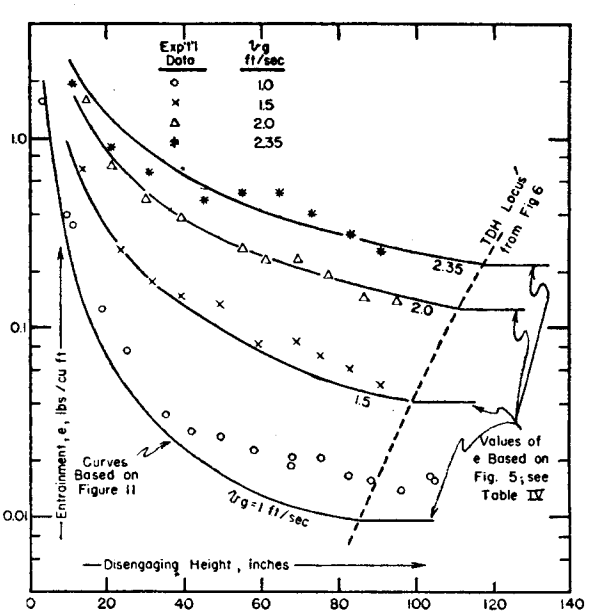

Fig. 10. Comparison between calculated and experimental entrainment data.

broken down into a sufficient number of components, both procedures should give the same result. In general, 3*b* is simpler, quicker, and less subject to the errors of insufficient component breakdown.

5. Divide the result from step 4 by the superficial gas velocity to obtain the entrainment rate in terms of pounds/cubic feet at T.D.H.

The particle-size breakdown and calculations for the superficial velocities of 1, 1.5, 2 and 2.35 ft./sec. are summarized in Table 2 and the results for all four experimental velocities are shown in comparison with the experimental data in Figure 10. In these calculations the standard drag coefficient for spheres was used to calculate the balancing velocity, the effects of any interparticle forces or of turbulence based on vessel dimensions being thus neglected.

Table 1. Entrainment of Typical Fluid Catalytic Cracking Catalyst (Figure 9) from an Air Fluidized Bed 2 in. × 24 in. in Cross-Section (Figure 8)

v_g = 1.0 ft./sec.		v_g = 1.5 ft./sec.		v_g = 2.0 ft./sec.		v_g = 2.35 ft./sec.	
Height above bed, in.	Entrainment lb./cu. ft.	Height above bed, in.	Entrainment lb./cu. ft.	Height above bed, in.	Entrainment lb./cu. ft.	Height above bed, in.	Entrainment lb./cu. ft.
105	0.0150	100	0.040	95	0.14	91	0.26
104	0.0160	91	.049	86	.145	83	.31
96	0.0138	83	.061	77	.19	73	.40
88	0.0152	75	.072	69	.23	65	.52
82	0.0163	69	.085	61	.23	55	.52
75	0.0205	60	.082	57	.265	45	.48
68	0.0205	50	.137	39	.39	31	.68
67	0.0184	39	.15	30	.49	21	.90
58	0.0225	31	.18	21	.72	12	2.0
50	0.0265	24	.26	14	1.60		
42	0.0280	14	.68				
35	0.035						
26	0.075						
19	0.122						
11	0.34						
9	0.39						
4	1.5						

VELOCITY DISSIPATION AND ENTRAINMENT BELOW T.D.H.

The curves drawn through the data of Figure 10 are based on an analogy with the velocity dissipation from gas jets. The curves are shown merely to illustrate the possibilities of this approach. The surface of the bed may be considered as a plane in which are located a number of nozzles which intermittently jet gas into the space above. The nozzles represent gas bubbles bursting at the bed surface. As a first approximation it was suggested that the distance required to dissipate continuous gas jets into space be considered as analogous. Koestel et al. (*6*) presented the results of such a study using ventilating ducts. Their data correlated as

$$\frac{V_x}{V_0} = 7\,\frac{\sqrt{A_c}}{X} \qquad (20)$$

Equation (20) applies to a situation in which the jet velocity dissipates into essentially infinite space and V_x approaches zero. In the case of bubble-velocity dissipation above a fluidized bed V_x, or in this instance V_{ge}, approaches v_g. Therefore, in order to converge to a finite value Equation (20) may be modified to read

$$\frac{V_x - v_g}{V_0} = \frac{(\text{constant})\cdot\xi(D_B)}{X} \qquad (21)$$

when the cross-sectional area of the orifice, A_c, is considered proportional to some function of the emerging bubble diameter.

Equation (21) is plotted in Figure 11 as V_x/V_0 for the case where v_g = 1.0 ft./sec. and V_0 = 12 ft./sec. The plotted points refer to the coordinates V_{ge}/V_g, vs. (height above bed)/T.D.H. and represent the velocity dissipation function derived from the data points of Figure 10. The curve in Figure 11, in conjunction with the correlation presented in Figure 5, was used to calculate the curves drawn through the original data in Figure 10.

Table 2. Illustration of Entrainment Transport Calculation

From Fig. 9 D, in.	wgt. fract., f	Calc'd. terminal velocity ft./sec.	50% point $D_{avg.}$, ins.	V_{ch}	$\frac{V_{ch}^2}{gD\rho^2}$	From Fig. 5 $W/V_{ch}P_0$	Calculated Entrainment $e = (W/V_{ch})\sum f$ lb./cu. ft.
0.00045	0.01	0.0226					
0.00066	.01	.0485					
0.00084	.03	.0799					
0.0011	.05	.138					
0.00137	.10	.216					
0.00168	.10	.320					
0.00194	.10	.421					
0.00218	.10	.507					
0.00246	.10	.628					
0.0028	.10	.799					
0.00318	.10	.99					
0.0037	.10	1.25	0.002	1.0	0.0154	0.16	0.0095
0.00435	.05	1.596	.00215	1.5	.0321	0.55	.04
0.0051	.03	1.99	.0022	2.0	.0560	1.7	.126
0.0066	.02	2.83	.0023	2.35	.0735	2.8	.213
tube blown clear		3.25					

The analogy to velocity dissipation from jets as represented by Equation (21) and Figure 11 is referred to here merely as an illustration of the relatively reasonable nature of such an approach. A far better procedure would be to develop the velocity dissipation function from experimental entrainment data using the theoretical approach through Equations (6) and (8). For significant results a larger variety of entrainment data such as shown in Figure 10 must be obtained for various particle sizes and densities.

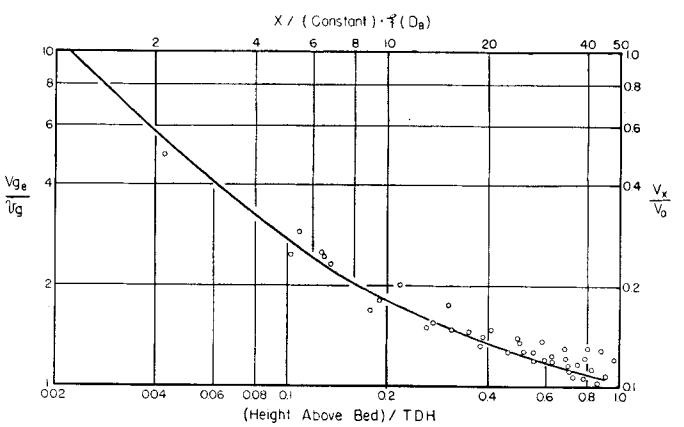

Fig. 11. Comparison between the bubble velocity dissipation function derived from entrainment data and the modified jet velocity dissipation function [Equation (21)].

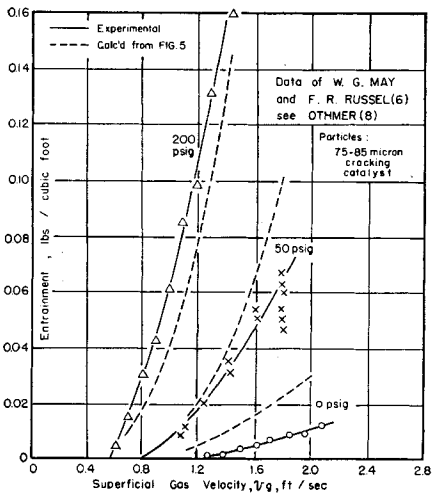

Fig. 12. Comparison between calculated and experimental entrainment at various fluidizing gas-pressure levels.

It is interesting to note that the analogy of Figure 11 indicates probable bubble velocities at the bed surface of about ten times the superficial velocity.

EFFECT OF HIGH-PRESSURE OPERATION

May and Russel (7) discussed the results of studies of the effect of high pressures on entrainment from beds of narrow- and wide-cut samples of FCC catalyst. Their data on a narrow-cut sample are given in Figure 12 as presented by Gohr (9). The solid curves are based on the experimental points; the dashed curves were computed from Figure 5. The agreement is not exceptional, but it does show rather well the proper order of the pressure effect. There is, of course, no assurance that any or all the experimental data were taken at distances above the bed greater than the transport disengaging height. It is also probable that the narrow diameter of the test vessel (2 in.) may have reduced its efficiency as a solids feeder particularly at low pressures where approach to slugging conditions may have occurred.

CONCLUSIONS

A mechanism of entrainment based on an effective bubble-velocity dissipation from the bed surface to the superficial velocity, at the transport disengaging height, has been developed. It has been shown to give fair agreement with representative entrainment data when correlated empirically and to yield curves of the form corresponding to experimental measurements when treated theoretically through a summation of force balances on the individual particles comprising the bed. Entrainment data from a minimum size experimental apparatus, represented as giving results which may be extrapolated to larger scale plants, have been presented for a typical fluid cracking catalyst, fluidized with atmospheric air. Published data at pressures up to 200 lb./sq. in. gauge are also shown in relatively good agreement with the proposed mechanism of entrainment. It is expected that with sufficient data application of the theory will permit deriving a velocity dissipation function, which in conjunction with particle force balances will predict the entrainment curves for any system.

NOTATION

A = effective particle cross-sectional area
A_c = cross-sectional area of jet nozzle at outlet
C = defined in text as $4\rho D^2/3\ k\mu$
C_R = coefficient of drag resistance
D = effective particle diameter
D_B = diameter of gas bubbles
D_T = tube or vessel diameter
E = entrainment, number of particles per unit volume of gas
e = entrainment, weight of particles per unit volume of gas
F = drag force
f = weight fraction of each component particle size in a mixture
g = gravitational constant
h = height above bed
h_{max} = maximum height of rise of particle above bed
K = entrainment multiplication or correction factor; ratio of true to calculated relative entrainment
k = particle shape factor (depends also on flow field)
m = particle mass
N = total number of particles thrown up from bed per unit bed cross-sectional area
n = number of particles of a given size thrown up from the bed per unit cross-sectional area
$\bar{n}$ = number or weight percentage of a given particle size in total spectrum
R = resistance of particle in motion
t = time
t^* = time taken to reach maximum height of rise
$\bar{t}$ = particle residence time above a given elevation
T.D.H. = transport disengaging height, height above bed at which entrainment equals saturation carrying capacity of gas stream
V_B = velocity of rise of gas bubbles
V_{ch} = superficial gas velocity taken at solids rate W_{ϵ_s} and voidage ϵ_s; or minimum gas velocity capable of carrying solids at rate W_{ϵ_s} in vertical upflow
V_{ge} = effective superficial gas velocity below T.D.H.
V_c = center-line gas velocity issuing from orifice
V_S = minimum gas velocity capable of carrying solids at rate W in horizontal flow
V_x = center-line gas velocity at distance X from orifice
V_{ϵ_s} = superficial gas velocity taken at particle inventory of $(1 - \epsilon_s)$ but with zero net flow of particles, for example, $W = 0$; or balancing velocity for suspension of voidage ϵ_s.
v = particle velocity
v_g = superficial gas velocity
v_m = particle balancing velocity
v_0 = particle velocity leaving bed surface
W = solids net flow rate per unit of tube cross-sectional area
W_{ϵ_s} = weight rate of upflow of total blend of particle size per unit of vessel cross-sectional area at the saturation voidage ϵ_s.
w_{ϵ_s} = uniform particle weight rate of upflow per unit of vessel cross-sectional area at the saturation voidage ϵ_s
X = distance from gas jet measured along center line normal to plane of the orifice

Greek Letters

ϵ_s = tube fractional voidage at saturation solids upflow rate
ρ = particle density
ρ_0 = fluid density
μ = fluid viscosity
ξ = arbitrary function

LITERATURE CITED

1. Ambrose, H. H., Ph.D. thesis, Univ. Iowa (1952); see also reference (7).
2. Blatch, N. S., *Trans. Am. Soc. Civil Engrs.*, **LVII**, 400 (1906).
3. Bond, R. K., *Chem. Eng.*, **64**, No. 10, 249 (1957).
4. Gregory, W. B., *Mech. Eng.*, **49**, 609 (1947).
5. Howard, G. W., *Proc. Am. Soc. Civil Engrs.*, **64**, 1377 (1938).
6. Koestel, A. E., P. Hermann, Tuve, G. L., *Heating, Piping Air Conditioning*, **22**, 113 (1950).
7. May, W. G., and F. R. Russel, paper presented at the North Jersey section of the A.C.S. (Jan. 25, 1954).
8. McNown, J. S., and M. C. Boyer, Proc. of the Fifth Hydraulics Conference, State Univ. Iowa Studies in Eng. Bull., 34 (1952).
9. Othmer, D. F., "Fluidization," Reinhold Pub. Co., N. Y. (1956).
10. Settle, J. J., R. Parkins, I.C.I. Ltd., General Chemicals Division, private communication (1951); see reference (*12*).
11. Smith, R. A., G. A. Carruthers, I.C.I. Ltd., Billingham Division, private communication (1951); see reference (*12*).
12. Spells, K. E., *Trans. Inst. Chem. Engrs. (London)*, **33**, No. 2, 79 (1955).
13. Thomas, D. G., Doc. 7540, Tech. Info. Div. U. S. Atomic Energy Comm., Oak Ridge, Tenn.
14. Yufin, A. P., *Izvest. U-Ser. Tekh. Nauk.*, No. 8, 1146 (1949).
15. Zenz, F. A., *Ind. Eng. Chem.*, **41**, 2801 (1949); see also reference (*9*).
16. Zenz, F. A., *Petroleum Refiner*, **36**, No. 6, 141 (1957).

Manuscript received August 13, 1957; revision received December 20, 1957; accepted January 6, 1958.